

# The first 1,3,2-diazaboro-[3]ferrocenophanes – molecular structures and dynamic behaviour in solution

Bernd Wrackmeyer<sup>\*</sup>, Elena V. Klimkina, Heidi E. Maisel,  
Wolfgang Milius, Max Herberhold<sup>\*</sup>

Laboratorium für Anorganische Chemie, Universität Bayreuth, Lehrstuhl f. Anorganische Chemie II, Universitätsstr. 30, NW 1,  
Bayreuth D-95440, Germany

Received 6 June 2003; accepted 2 September 2003

Dedicated to Professor Helmut Werner on the occasion of his 70th birthday

## Abstract

Dilithiated 1,1'-bis(trimethylsilylamino)ferrocene (**1**) reacts with aminoboron dihalides (**2**)  $X_2B-N(R')R$  [ $X = Br$ ,  $R' = R = Et$  (**2a**);  $X = Cl$ ,  $R' = Me$ ,  $R = CH_2Ph$  (**2b**),  $X = Cl$ ,  $R' = Et$ ,  $R = Ph$  (**2c**)] to give 2-amino-1,3,2-diazaboro-[3]ferrocenophanes (**3a–c**) for the first time. The steric constraints exerted by the [3]ferrocenophane unit and the presence of the  $N-SiMe_3$  groups cause rather different B–N bonding situations in these tri(amino)boranes. The boron atom has the choice between three nitrogen atoms for  $BN(pp)\pi$  bonding: in the cases of **3a** and **3b**, it prefers the  $NEt_2$  and the  $N(Me)CH_2Ph$  group, respectively, over the  $N-SiMe_3$  groups, whereas in **3c** the  $N(Et)Ph$  group appears to be the weaker  $\pi$ -donor. This can be concluded from the X-ray structural analyses carried out for **3a** and **3c**, and from the low temperature  $^1H$ ,  $^{13}C$ , and  $^{29}Si$  NMR spectra of **3a–3c**.  
© 2003 Elsevier B.V. All rights reserved.

**Keywords:** Ferrocene; Boron; NMR – multinuclear; X-ray

## 1. Introduction

Recently, the chelating ability of the 1,1'-bis(trimethylsilylamino)ferrocene ligand has been established for magnesium, titanium [1,2], zirconium [1], and tin derivatives [3,4]. The ring closure to the 1,3,2-diazahetero-[3]ferrocenophane system enforces an approximately perpendicular orientation of the lone electron pairs at both nitrogen atoms with respect to the  $\pi$  system of the cyclopentadienyl rings (Scheme 1; **A–C**). In this context, a boron atom with trigonal planar surroundings in the central 2-position of the bridge could be an attractive probe for studying  $\pi$  interactions of the boron  $p_z$  orbital with the lone pairs of electrons at the nitrogen atoms [5–8], in particular if the boron atom is linked to a third amino group as in **A–C** (Scheme 1). Depending on

the nature of the substituents  $R$  and  $R'$  in the exocyclic amino group, the boron atom may prefer either the exocyclic  $BN(pp)\pi$  bonding (**B**) with considerable distortion of the [3]ferrocenophane structure or the endocyclic  $BN(pp)\pi$  interactions (**C**), where the boron atom lies in the plane formed by  $Fe$ ,  $C(1)$ ,  $C(1')$  and the two nitrogen atoms. The structure **A** with perfect  $BN(pp)\pi$  bonding involving all three nitrogen atoms is unlikely, since the bulky  $N-SiMe_3$  groups will prevent an appropriate orientation of the exocyclic amino group  $N(R)R'$ . In the present work, we describe the synthesis of the first three examples of 1,3,2-diazaboro-[3]ferrocenophanes and their structural characterisation.

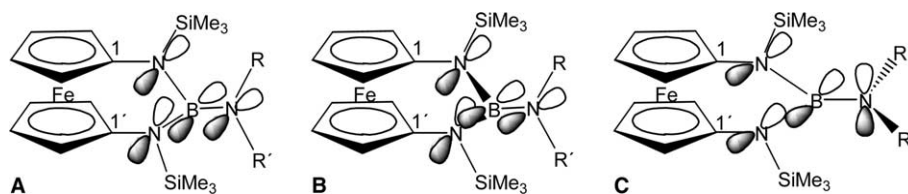
## 2. Results and discussion

### 2.1. Synthesis of the 1,3,2-diazaboro-[3]ferrocenophanes

In general, dilithiation of 1,1'-bis(trimethylsilylamino)ferrocene proceeds readily [1,3,9] to give **1** which

<sup>\*</sup> Corresponding authors. Tel.: +49-921-55-2542; fax: +49-921-55-2157 (B. Wrackmeyer); fax: +49-921-55-2157 (M. Herberhold).

E-mail addresses: [b.wrack@uni-bayreuth.de](mailto:b.wrack@uni-bayreuth.de) (B. Wrackmeyer), [max.herberhold@uni-bayreuth.de](mailto:max.herberhold@uni-bayreuth.de) (M. Herberhold).

Scheme 1. BN(pp) $\pi$  interactions in 2-amino substituted 1,3,2-diazabora-[3]ferrocenophanes.

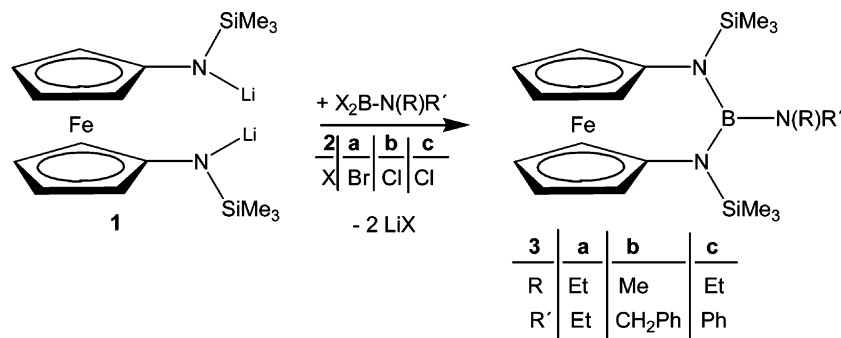
may then react with element halides to afford the corresponding [3]ferrocenophanes. Although the magnesium derivative sometimes gives better results [1,3], treatment of **1** with different aminoboron dihalides (**2**) (Scheme 2) provides a fairly straightforward route to the desired 1,3,2-diazabora-[3]ferrocenophanes (**3**).

The tri(amino)boranes (**3**) are orange solids (**3a**, **3c**) or an orange oil (**3b**) which are very sensitive towards traces of moisture. Their solutions in benzene, toluene,  $\text{CDCl}_3$  or  $\text{CD}_2\text{Cl}_2$  cannot be kept for prolonged periods at room temperature without decomposition. In contrast to **3a** which is obtained in high yield and can be readily purified by crystallisation, the formation of **3b** and **3c** is accompanied by side reactions, and the crystallisation of pure products is slow. The side reactions involve the formation of bis(amino)boron chlorides

$[\text{R}'(\text{R})\text{N}]_2\text{B-Cl}$ , and presumably also of the 2-chloro-1,3,2-diazabora-[3]ferrocenophane [10]. Suitable crystals for X-ray structural analysis were obtained for **3a** and **3c** (vide infra). All three complexes **3a–3c** were sufficiently soluble in  $\text{CDCl}_3$ ,  $\text{CD}_2\text{Cl}_2$  or toluene for NMR studies at low temperature. These measurements revealed structural details corresponding to the solid-state structures in the cases of **3a** and **3c**, and in the case of **3b** at low temperature the bonding situation is comparable to that found for **3a**.

## 2.2. NMR spectroscopic results

Fig. 1 shows a typical one-dimensional NOE experiment [11] carried out for **3a** which confirms the assignment of the  $^1\text{H}(\text{C}_5\text{H}_4)$  NMR signals. The broadened



Scheme 2. Synthesis of the 1,3,2-diazabora-[3]ferrocenophanes.

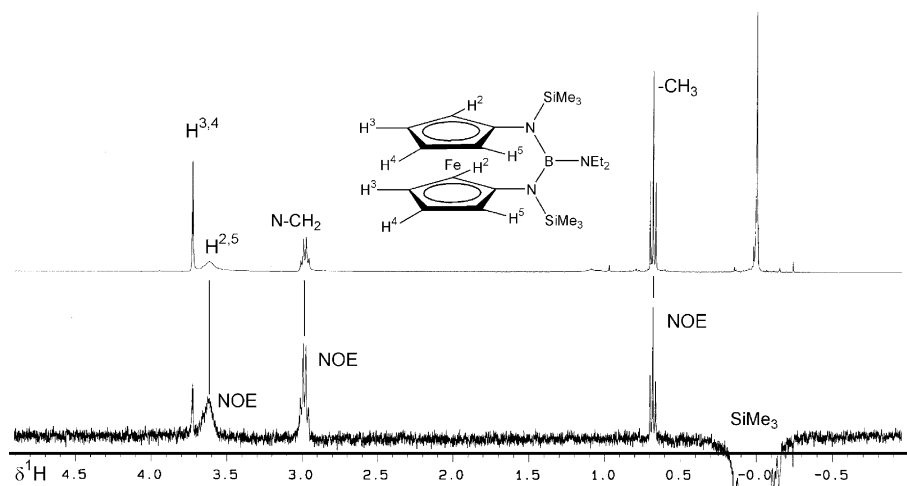


Fig. 1. The 500.13 MHz  $^1\text{H}/^1\text{H}$  NOE difference spectrum of **3a** (in  $\text{C}_6\text{D}_6$  at 23 °C), using the gradient-enhanced version of the experiment [11b]. The transitions of the N-SiMe $_3$  groups are irradiated, and the response is indicated. Note the broad  $^1\text{H}^{2,5}$  NMR signals.

$^1\text{H}^{2,5}$  NMR signal indicates a dynamic process, of which the origin is not obvious at first glance. At lower temperature, the pairwise degeneracy of the  $^1\text{H}^{2,5}$ ,  $^1\text{H}^{3,4}$  and, better resolved, of the  $^{13}\text{C}^{2,5}$  and  $^{13}\text{C}^{3,4}$  NMR signals is lifted, giving rise to four signals instead of two in both the  $^1\text{H}$  and  $^{13}\text{C}$  NMR spectra. At the lowest temperature studied in the case of **3a** ( $-70^\circ\text{C}$ ), the signals of the  $\text{NEt}_2$  group ( $^1\text{H}$ ,  $^{13}\text{C}$  NMR) and of the  $\text{NSiMe}_3$  groups ( $^1\text{H}$ ,  $^{13}\text{C}$ ,  $^{29}\text{Si}$  NMR) remain unchanged. It can be concluded, as in structure **B**, that rotation about the exocyclic B–N bond is slow, and that the boron atom is shifted out of the plane defined by Fe, C(1), C(1') and the two nitrogen atoms, which explains the appearance of the  $\text{C}_5\text{H}_4$  NMR signals. Structure **B** requires that the ethyl ( $\text{NEt}_2$ ) groups and the N– $\text{SiMe}_3$  substituents remain equivalent, in agreement with the NMR spectra. The activation energy of the hindered rotation about the exocyclic B–N bond can be evaluated from the  $^{13}\text{C}$  NMR spectra [12]. The magnitude of  $\Delta G_{(0^\circ\text{C})}^\ddagger = 58 \pm 1$  kJ/mol is much higher than for other tri(amino)boranes and lies in the range more typical of amino(diorgano)boranes [13a,13b].

Inspection of the NMR spectra of **3b** reveals broadened signals at room temperature in all regions. At low temperature, the signals become sharp, and the  $\text{C}_5\text{H}_4$  groups exhibit 10  $^{13}\text{C}$  NMR signals (Fig. 2, lower trace). Since there are also two  $^{29}\text{Si}$  NMR signals, we are dealing again with a structure of type **B**. The hindered rotation about the exocyclic B–N bond becomes apparent from the complete loss of molecular symmetry, as indicated by the  $^1\text{H}$  and  $^{13}\text{C}$  NMR signals of the  $\text{C}_5\text{H}_4$  groups and the observation of two  $^{13}\text{C}$  and  $^{29}\text{Si}$  NMR signals for the N– $\text{SiMe}_3$  groups. The presence of two different substituents at nitrogen in **3b**, in contrast to **3a**, leaves no doubt with regard to restricted rotation about the exocyclic B–N bond in **3b**, and it is therefore rea-

sonable to assume efficient exocyclic  $\text{BN}(\text{pp})\pi$  bonding in both **3a** and **3b**.

Finally, the case of **3c** is different, although at first sight it might be tempting to assume a situation analogous to that found for **3b**. However, all NMR spectroscopic evidence in solution at low temperature indicates that a plane of symmetry is present in the molecular structure of **3c**, in contrast to the situation in **3b**. There is only one  $^1\text{H}$ ,  $^{13}\text{C}$  and  $^{29}\text{Si}$  NMR signal for the two N– $\text{SiMe}_3$  groups in **3c**, and there are four  $^1\text{H}$  and  $^{13}\text{C}(\text{CH})$  NMR signals, respectively, for the  $\text{C}_5\text{H}_4$  groups (Fig. 2, upper trace). This means that the boron atom lies in the Fe, C(1), C(1'), N, N plane as in structure **C**, and that the amino group cannot freely rotate, most likely for steric reasons. The observation of two  $^{13}\text{C}(\text{ortho})$  and two  $^{13}\text{C}(\text{meta})$  signals for the N–Ph group at low temperature is the result of hindered rotation about the N–C(*ipso*) bond [13b,13c]. This particular structural feature supports the assumption that the phenyl group competes successfully as a  $\pi$  acceptor for the  $\pi$  electron density at the exocyclic nitrogen atom. The electron deficiency of the boron atom in **3c** is then mainly compensated, in contrast to the situation in **3a** and **3b**, by endocyclic  $\text{BN}(\text{pp})\pi$  interactions.

The  $\delta^{11}\text{B}$  values of **3a–3c** lie in the range typical of tri(amino)boranes bearing N– $\text{SiMe}_3$  and/or N-aryl groups [14], and since they represent the sum of all interactions, they cannot be used straightforwardly to discuss differences in  $\text{BN}(\text{pp})\pi$  bonding. There is no systematic study of  $^{29}\text{Si}$  NMR data of N-silylamino-boranes available. In the light of the present results such measurements appear to be rewarding considering the marked difference in  $^{29}\text{Si}$  nuclear shielding between **3a**, **3b** ( $\delta^{29}\text{Si} = 1.0, 1.9$ ) on the one side and **3c** ( $\delta^{29}\text{Si} = 8.4$ ) on the other side. In the former cases  $\text{BN}(\text{pp})\pi$  bonding is weak for the N– $\text{SiMe}_3$  groups in contrast to the latter

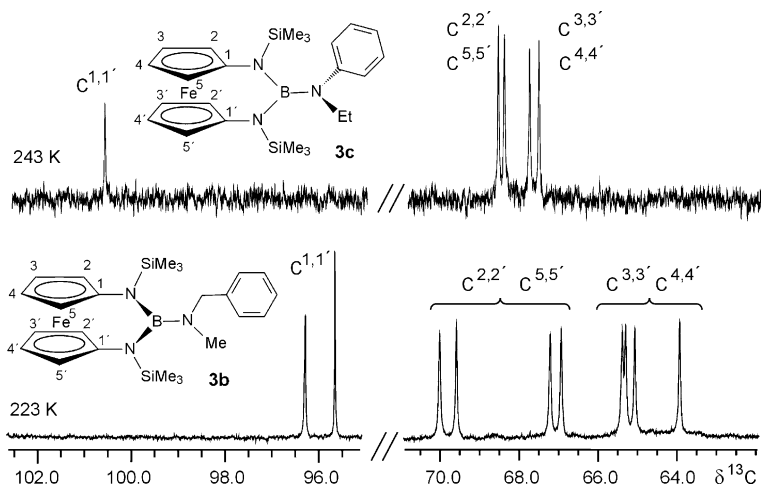


Fig. 2. Parts of the low temperature 62.9 MHz  $^{13}\text{C}\{^1\text{H}\}$  NMR spectra of the [3]ferrocenophanes (**3b**) (lower trace) and (**3c**) (upper trace). Note the complete loss of symmetry in the case of **3b** [10  $^{13}\text{C}(\text{C}_5\text{H}_4)$  signals] in contrast to **3c** [five  $^{13}\text{C}(\text{C}_5\text{H}_4)$  signals].

Table 1  
 $^{11}\text{B}$ ,  $^{13}\text{C}$ , and  $^{29}\text{Si}$  NMR data<sup>a</sup> of the 2-amino-1,3-bis(trimethylsilyl)-1,3,2-diazaboro-[3]ferrocenophanes (**3**)

Compound N(R)R'	<b>3a</b> , NEt <sub>2</sub>		<b>3b</b> , N(Me)CH <sub>2</sub> Ph		<b>3c</b> , N(Et)Ph	
	23 °C	−50 °C <sup>b</sup>	23 °C	−50 °C	23 °C	−30 °C
$\delta^{13}\text{C}(\text{N-SiMe}_3)$	1.4 (57.0)	1.2	1.5 (56.5)	0.7 (56.8) 0.8 (56.8)	2.2 (57.7)	2.0 (57.3)
$\delta^{13}\text{C}(\text{NR})$	39.6, 13.7	39.0, 13.5	36.5	35.6	12.9 40.9 (br)	12.7 40.4
$\delta^{13}\text{C}(\text{NR}')$	39.6, 13.7	39.0, 13.5	55.7 (CH <sub>2</sub> ) 127.2 128.2 128.9 139.8	54.6 (CH <sub>2</sub> ) 126.5 (C <sub>p</sub> ) 127.2 128.3 139.1 (C <sub>i</sub> )	109.9 (br) 115.2 116.3 (br) 128.3 (br) 128.9 (br) 149.9	109.5 (C <sub>o</sub> ) 114.5 (C <sub>p</sub> ) 115.8 (C <sub>o</sub> ) 128.1 (C <sub>m</sub> ) 129.2 (C <sub>m</sub> ) 149.7 (C <sub>i</sub> )
$\delta^{13}\text{C}(\text{fc-C}^1)$	96.3	95.9	96.6	96.2, 95.6	101.2	100.9
$\delta^{13}\text{C}(\text{fc-C}^{2,5})$	67.0 (br)	70.3, 67.8	66.8 (br)	70.1, 69.6 67.3, 67.0	68.8	68.7, 68.6
$\delta^{13}\text{C}(\text{fc-C}^{3,4})$	67.0 (br)	66.3, 64.9	66.8 (br)	65.44, 65.36 65.1, 64.0	67.9	67.9, 67.7
$\delta^{11}\text{B}$	27.8		28.6		31.0	
$\delta^{29}\text{Si}$	1.0		1.9 (56.8)	2.2 (56.6) 2.7 (56.4)	8.4 (57.7)	

<sup>a</sup> Measured in C<sub>6</sub>D<sub>6</sub> (**3a**), CD<sub>2</sub>Cl<sub>2</sub> (**3b**), CDCl<sub>3</sub> (**3c**); coupling constants  $J(^{29}\text{Si}, ^{13}\text{C})$  ( $\pm 0.5$  Hz) are given in parentheses.

<sup>b</sup> In [D<sub>8</sub>]toluene at −50 °C.

case. There are also considerable differences in the respective B–N and N–Si bond lengths and in the bond angles at the N(Si) atoms (vide infra) (see Table 1).

### 2.3. Molecular structures of the [3]ferrocenophanes (**3a**) and (**3c**)

The molecular structures of complexes **3a** and **3c** are shown in Figs. 3 and 4, respectively. Selected bond lengths and angles are given in Table 2. The surroundings of the boron and nitrogen atoms are trigonal planar

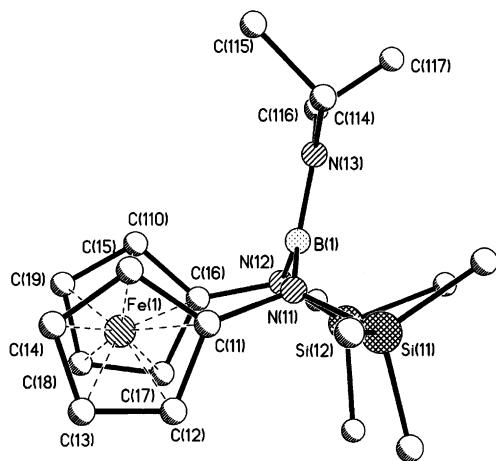


Fig. 3. Molecular structure of **3a** showing the non-planar [3]ferrocenophane ring as the result of efficient exocyclic BN(pp) $\pi$  bonding which is also evident from the respective B–N bond lengths (Table 2).

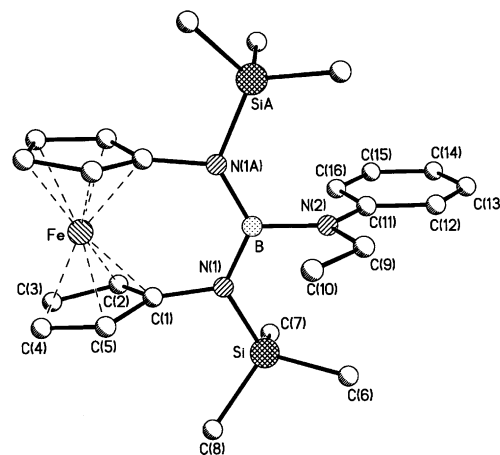


Fig. 4. Molecular structure of **3c**. The boron atom lies in the plane formed by Fe, C(1), and N(1) as the result of efficient endocyclic BN(pp) bonding (see Table 2) and perpendicular arrangement of the NC(9)C(11) plane with respect to the N(1)BN(1A) plane.

within the experimental error. The shape of the ferrocenophane ring in **3a** indicates weak endocyclic and strong exocyclic BN(pp) $\pi$  bonding, confirmed by the presence of fairly long [7,8] endocyclic B–N bonds and a rather short [7,8] exocyclic B–N bond. The opposite situation is found for the molecular structure of **3c**, where the endocyclic B–N bonds are short and the exocyclic B–N bond is long, in agreement with the arrangement of the plane of the exocyclic amino group with respect to the ferrocenophane ring.

Table 2  
Selected bond lengths (pm) and angles ( $^{\circ}$ )<sup>a</sup> of the [3]ferrocenophanes (**3a**) (Fig. 3) and (**3c**) (Fig. 4)

<b>3a</b>		<b>3c</b>	
C(11)–N(11)	142.3(7)	C(1)–N(1)	1.446(3)
C(16)–N(12)	142.8(8)	N(1)–B	1.446(3)
N(11)–B(1)	147.0(9)	N(2)–B	149.2(6)
N(12)–B(1)	151.2(9)	N(1)–Si(1)	179.2(3)
N(13)–B(1)	140.1(9)	N(2)–C(9)	146.2(5)
N(11)–Si(11)	171.9(5)	N(2)–C(11)	138.7(5)
N(12)–Si(12)	170.7(5)	Fe···B	342.6
N(13)–C(114)	148.6(7)	C(1)–Fe–C(1A)	94.8(2)
N(13)–C(116)	146.5(8)	Fe–C(1)–N(1)	125.9(2)
Fe(1)···B(1)	316.4	C(1)–N(1)–Si(1)	108.5(2)
C(11)–Fe(1)–C(16)	96.9(3)	N(1)–B–N(1A)	126.7(4)
Fe(1)–C(11)–N(11)	122.5(4)	N(1)–B–N(2)	116.6(2)
Fe(1)–C(16)–N(12)	122.2(4)	C(11)N(2)C(9)/N(1)B(N(1A))	90
C(11)–N(11)–Si(11)	116.0(4)	C <sub>5</sub> /C <sub>5</sub> ( $\alpha$ )	15.0
C(16)–N(12)–Si(12)	120.7(4)	C <sub>5</sub> /N(1) ( $\beta$ )	0.9
N(11)–B(1)–N(12)	121.0(6)	C <sub>5</sub> –Fe–C <sub>5</sub> ( $\gamma$ )	170.3
N(11)–B(1)–N(13)	120.4(7)	C <sub>5</sub> /C <sub>5</sub> (twist) ( $\tau$ )	0 (symmetry)
N(12)–B(1)–N(13)	118.5(7)		
C(114)N(13)C(116)/N(11)BN(12)	171.8		
C <sub>5</sub> /C <sub>5</sub> ( $\alpha$ )	10.8		
C <sub>5</sub> /N(11) ( $\beta_1$ )	4.5		
C <sub>5</sub> /N(12) ( $\beta_2$ )	3.8		
C <sub>5</sub> –Fe(1)–C <sub>5</sub> ( $\gamma$ )	170.6		
C <sub>5</sub> /C <sub>5</sub> (twist) ( $\tau$ )	0.7		

<sup>a</sup> The definition of the angles  $\alpha$ ,  $\beta$ ,  $\gamma$  and  $\tau$  is given in [16b,16c].

There are also marked differences in the N–Si bond lengths in **3a** and **3c**, being short [15] in **3a** and long in **3c**. It is tempting to relate these features to the availability of the lone pairs of electrons at the N(Si) nitrogen atoms for additional Si–N bonding interactions, since the degree of BN(Si)(pp) $\pi$  bonding is low in **3a** and high in **3c**.

The cyclopentadienyl rings in the structures of both **3a** and **3c** lie almost exactly in eclipsed positions, as in many other [*n*]ferrocenophanes with *n* = 1, 2 [16] and *n* = 3 [1–4,16], somewhat tilted against a parallel arrangement (see angles  $\alpha$  and  $\gamma$  in Table 2) towards the NBN unit. However, the mutual positions of the cyclopentadienyl rings (staggered, eclipsed or in between) depend strongly on the geometry and nature of the bridge, as is evident for the molecular structures of various [3]ferrocenophanes [17]. As a result of the different ferrocenophane ring geometries, the non-bonding Fe···B distances differ markedly in **3a** and **3c**.

### 3. Conclusions

The molecular structures both in solution and in the solid state of the first 1,3,2-diazaboro-[3]ferrocenophanes (**3a–c**) depend on a remarkable manner on the nature of the amino group in 2-position. Strong  $\pi$  donors such as the NEt<sub>2</sub> (**3a**) or N(Me)CH<sub>2</sub>Ph groups (**3b**) enforce a nonplanar ferrocenophane ring whereas weaker  $\pi$  donors such as a N(Et)Ph group induces efficient endocyclic BN(pp) $\pi$  bonding for which a planar [3]ferrocenophane ring is required as in **3c**.

## 4. Experimental

### 4.1. General

The preparation and handling of all compounds were carried out in an atmosphere of dry argon and carefully dried solvents were used throughout. Starting materials were prepared as described (1,1'-bis(trimethylsilylamino)ferrocene [**1b**]), diethylaminoboron dibromide (**2a**) from BBr<sub>3</sub> and B(NEt<sub>2</sub>)<sub>3</sub> (molar ratio 2:1), benzyl(methyl)aminoboron dichloride (**2b**) [18] and ethyl(phenyl)aminoboron dichloride (**2c**) [18]. Other starting materials were commercially available, such as *n*-butyllithium (1.6 M in hexane) and boron trichloride (1.0 M in hexane). NMR measurements: Bruker ARX 250 and Bruker DRX 500: <sup>1</sup>H, <sup>11</sup>B, <sup>13</sup>C, <sup>29</sup>Si NMR (refocused INEPT [19] based on <sup>2</sup>J(<sup>29</sup>Si, <sup>1</sup>H) = 7 Hz); chemical shifts are given with respect to Me<sub>4</sub>Si [ $\delta^1$ H (CHCl<sub>3</sub>/CDCl<sub>3</sub>) = 7.24;  $\delta^{13}$ C (CDCl<sub>3</sub>) = 77.0, (CD<sub>2</sub>Cl<sub>2</sub>) = 53.5, (C<sub>6</sub>D<sub>6</sub>) = 128.0, (C<sub>6</sub>D<sub>5</sub>CD<sub>3</sub>) = 20.5;  $\delta^{29}$ Si = 0 for  $\Xi$ (<sup>29</sup>Si) = 19.867184 MHz]; external BF<sub>3</sub>-OEt<sub>2</sub> [ $\delta^{11}$ B = 0 for  $\Xi$ (<sup>11</sup>B) = 32.083971 MHz].

### 4.2. Synthesis of the N,N'-dilithioamide **1** (fc(NSiMe<sub>3</sub>)<sub>2</sub>Li<sub>2</sub>)

A solution of fc(NHSiMe<sub>3</sub>)<sub>2</sub> (350 mg, 0.97 mmol) in hexane (25 mL) was cooled (–60 °C), and *n*-BuLi was added (1.21 mL of a 1.6 M solution in hexane, 1.94 mmol). The reaction mixture was stirred at –60 °C for 1

h, then allowed to reach ambient temperature and kept stirring for further 30 min. The formation of a red precipitate was observed which was separated using a centrifuge and decanting the supernatant liquid. The solid was dried under vacuum to give 340 mg (94%) of **1** as an orange powder.

#### 4.3. Properties of the aminoboron dichlorides (**2b**) and (**2c**)

Benzyl(methyl)aminoboron dichloride (**2b**): b.p. 40–42 °C/0.2 Torr ([20]; b.p. 68 °C/2 Torr). <sup>1</sup>H NMR (250.1 MHz; CDCl<sub>3</sub>; 25 °C): δ = 2.89 (s, 3H, MeN), 4.51 (s, 2H, NCH<sub>2</sub>), 7.25–7.50 (m, 5H, Ph). <sup>13</sup>C NMR (62.9 MHz; CDCl<sub>3</sub>; 25 °C): δ = 37.1 (MeN), 55.8 (NCH<sub>2</sub>), 127.6 (C<sub>o,p</sub>), 128.6 (C<sub>m</sub>), 137.0 (C<sub>i</sub>). <sup>11</sup>B NMR (80.3 MHz; CDCl<sub>3</sub>; 25 °C): δ = 31.3.

Ethyl(phenyl)aminoboron dichloride (**2c**): b.p. 38–39 °C/0.2 Torr ([21]; b.p. 67 °C/3 Torr). <sup>1</sup>H NMR (250.1 MHz; CDCl<sub>3</sub>; 25 °C): δ = 3.73, 1.14 (q, t, 5H, EtN), 7.05–7.20 (m, 2H, Ph), 7.25–7.50 (m, 3H, Ph). <sup>13</sup>C NMR (62.9 MHz; CDCl<sub>3</sub>; 25 °C): δ = 49.4, 14.4 (EtN), 126.9 (C<sub>p</sub>), 127.8 (C<sub>o</sub>), 129.2 (C<sub>m</sub>), 144.8 (C<sub>i</sub>). <sup>11</sup>B NMR (80.3 MHz; CDCl<sub>3</sub>; 25 °C): δ = 31.4.

#### 4.4. Synthesis of the 1,3-bis(trimethylsilyl)-2-amino-1,3,2-diazaborene-*[3]*ferrocenophanes (**3a**)–(**3c**)

2-Diethylamino-1,3-bis(trimethylsilyl)-1,3,2-diazaborene-*[3]*ferrocenophane (**3a**): Freshly prepared fc(NSiMe<sub>3</sub>)<sub>2</sub>Li<sub>2</sub> (**1**) (0.32 g, 0.86 mmol) was taken up in hexane (10 mL), and the suspension was cooled to –30 °C. After

adding a solution of Et<sub>2</sub>NBBR<sub>2</sub> (**2a**) (0.21 g, 0.8 mmol) in hexane (10 mL), the mixture was warmed to room temperature and kept stirring for 12 h. Insoluble materials were filtered off and the solvent was removed in vacuo. The residue, a yellow oil which slowly became solid, was dissolved in a small amount of hexane, and the solution was stored at –18 °C for several days. Then **3a** was obtained as orange crystals (0.31 g; 81%; m.p. 161 °C). <sup>1</sup>H NMR (500.1 MHz; C<sub>6</sub>D<sub>6</sub>; 25 °C): δ = 0.43 (s, 18H, Me<sub>3</sub>Si), 3.40, 1.10 (q, t, 10H, Et<sub>2</sub>N), 4.10 (br, 4H, H<sup>2,2',5,5'</sup>), 4.16 (m, 4H, H<sup>3,3',4,4'</sup>).

2-Benzyl(methyl)amino-1,3-bis(trimethylsilyl)-1,3,2-diazaborene-*[3]*ferrocenophane (**3b**): A suspension of fc(NSiMe<sub>3</sub>)<sub>2</sub>Li<sub>2</sub> (**1**) (100 mg, 0.27 mmol) in hexane (15 mL) was cooled to –70 °C, and PhCH<sub>2</sub>(Me)NBCL<sub>2</sub> (**2b**) (54 mg, 0.27 mmol) was injected slowly through a syringe. After stirring the reaction mixture for 1 h at –70 °C and then for 3 h at ambient temperature, the mixture was separated by centrifugation from insoluble materials, and the liquid was collected. Volatile materials were removed in vacuo (0.01 Torr), and the resulting oil was dissolved in hexane (15 mL). After filtration the solvent was removed in vacuo to give 85 mg (65%) of **3b** as a yellow-orange oil. <sup>1</sup>H NMR (CDCl<sub>3</sub>, 25 °C): δ = 0.23 (s, 18H, Me<sub>3</sub>Si), 2.72 (s, 3H, MeN), 3.83 (br), 3.90 (br) (m, 4H, H<sup>2,2',5,5'</sup>), 3.94 (m, 4H, H<sup>3,3',4,4'</sup>), 4.48 (br) (s, 2H, NCH<sub>2</sub>), 7.2–7.5 (m, 5H, Ph).

2-Ethyl(phenyl)amino-1,3-bis(trimethylsilyl)-1,3,2-diazaborene-*[3]*ferrocenophane (**3c**): The synthesis was carried out in analogy to that of **3b**, starting from 170 mg (0.46 mmol) of fc(NSiMe<sub>3</sub>)<sub>2</sub>Li<sub>2</sub> (**1**) and 92 mg (0.46 mmol) of Et(Ph)NBCL<sub>2</sub> (**2c**), to give 130 mg (58%) of **3c**

Table 3  
Crystallographic data of the *[3]*ferrocenophanes (**3a**) and (**3c**)

	<b>3a</b>	<b>3c</b>
Formula	C <sub>20</sub> H <sub>36</sub> BN <sub>3</sub> Si <sub>2</sub> Fe	C <sub>24</sub> H <sub>36</sub> BN <sub>3</sub> Si <sub>2</sub> Fe
Crystal	orange prism	orange platelet
Dimensions (mm)	0.18 × 0.15 × 0.12	0.18 × 0.16 × 0.06
Crystal system	triclinic	orthorhombic
Space group	<i>P</i> $\bar{1}$	<i>Pnma</i>
Lattice parameters (pm, °)	<i>a</i> = 1010.1(2) <i>b</i> = 2508.4(5) <i>c</i> = 3137.5(6) $\alpha$ = 70.10(3) $\beta$ = 89.94(3) $\gamma$ = 78.41(3)	<i>a</i> = 1547.2(3) <i>b</i> = 1393.9(3) <i>c</i> = 1223.6(2)
<i>Z</i>	12	4
Absorption coefficient $\mu$ (mm <sup>-1</sup> )	0.728	0.678
Diffractometer	STOE IPDS I (Mo K $\alpha$ , $\lambda$ = 71 073 pm), graphite monochromator	
Measuring range ( $\theta$ )	2–26	2–26
Reflections collected	48 042	18 381
Independent reflections ( <i>I</i> > 2 $\sigma$ ( <i>I</i> ))	6658 (26 006 all)	1130 (2612 all)
Absorption correction	none <sup>a</sup>	numerical
Refined parameters	1460	157
<i>wR</i> <sub>2</sub> / <i>R</i> <sub>1</sub> ( <i>I</i> > 2 $\sigma$ ( <i>I</i> ))	0.070/0.047	0.079/0.038
Maximum/minimum residual electron density (e pm <sup>-3</sup> 10 <sup>-6</sup> )	0.32/–0.19	0.40/–0.17

<sup>a</sup> Absorption correction did not improve the data set.

as a yellow oil. Crystallisation from hexane gave, after 2 months at  $-30\text{ }^{\circ}\text{C}$ , orange crystals of **3c**, m.p. 131–132  $^{\circ}\text{C}$ .  $^1\text{H NMR}$  ( $\text{CDCl}_3$ ,  $25\text{ }^{\circ}\text{C}$ ,  $J/\text{Hz}$ ):  $\delta = -0.12$  (s, 18H,  $\text{Me}_3\text{Si}$ ), 3.10, 1.40 (q, t, 5H, EtN), 3.83 (br), 3.90 (br) (m, 4H,  $\text{H}^{2,2',5,5'}$ ), 4.05 (m, 4H,  $\text{H}^{3,3',4,4'}$ ), 6.55 (br) (m, 2H, Ph- $\text{H}_o$ ), 6.62 (m, 1H, Ph- $\text{H}_p$ ), 7.17 (br) (m, 2H, Ph- $\text{H}_m$ ).  $^1\text{H NMR}$  ( $\text{CDCl}_3$ ,  $-30\text{ }^{\circ}\text{C}$ ):  $\delta = -0.17$  (s, 18H,  $\text{Me}_3\text{Si}$ ), 1.38 (t, 3H,  $\text{CH}_3$ ), 3.03 (q, 2H,  $\text{NCH}_2$ ), 3.78, 3.90 (m, m, 2H, 2H,  $\text{H}^{2,2',5,5'}$ ), 4.04 (m, 4H,  $\text{H}^{3,3',4,4'}$ ), 6.42 (m, 2H, Ph- $\text{H}_o$ ), 6.58 (m, 1H, Ph- $\text{H}_p$ ), 7.13 (m, 2H, Ph- $\text{H}_m$ ).

#### 4.5. Crystal structure determinations of the 2-amino-1,3,2-diazaborene-*[3]*ferrocenophanes (**3a**) and (**3e**)

Details pertinent to the crystal structure determinations are listed in Table 3. Crystals of appropriate size were sealed under argon in Lindemann capillaries. The data collections were carried out at  $20\text{ }^{\circ}\text{C}$ .

### 5. Supplementary information

Crystallographic data (excluding structure factors) for the structures reported in this paper have been deposited with the Cambridge Crystallographic Data Centre as supplementary publications no. CCDC-210104 (**3a**) and CCDC-210105 (**3e**). Copies of the data can be obtained free of charge on application to CCDC, 12 Union Road, Cambridge CB2 1EZ, UK [fax (internat.): +44 (0)1223/336033; [deposit@ccdc.cam.ac.uk](mailto:deposit@ccdc.cam.ac.uk)].

### Acknowledgements

This work was supported by the Deutsche Forschungsgemeinschaft and the Fonds der Chemischen Industrie.

### References

- [1] (a) A. Shafir, M.P. Power, G.D. Whitener, J. Arnold, *Organometallics* 19 (2000) 2987; (b) A. Shafir, M.P. Power, G.D. Whitener, J. Arnold, *Organometallics* 20 (2001) 1365; (c)cf. M. Herberhold, *Angew. Chem.* 114 (2002) 998; (d)cf. M. Herberhold, *Angew. Chem., Int. Ed. Engl.* 41 (2002) 956.
- [2] A. Shafir, J. Arnold, *J. Am. Chem. Soc.* 123 (2001) 9212.
- [3] B. Wrackmeyer, W. Milius, H.E. Maisel, H. Vollrath, M. Herberhold, *Z. Anorg. Allg. Chem.* 629 (2003) 1169.
- [4] B. Wrackmeyer, H.E. Maisel, W. Milius, M. Herberhold, *J. Organomet. Chem.* 680 (2003) 271.
- [5] (a) E. Wiberg, *Naturwissenschaften* 35 (1848) 182; (b) E. Wiberg, *Naturwissenschaften* 35 (1848) 212; (c) K. Niedenzu, J.W. Dawson, *Boron–Nitrogen Compounds*, Springer, Heidelberg, 1965, p. 48.
- [6] (a) H. Bock, W. Fuß, *Chem. Ber.* 104 (1971) 1687; (b) H.J. Becher, J. Goubeau, *Z. Anorg. Allg. Chem.* 268 (1967) 133; (c) H. Nöth, H. Vahrenkamp, *Chem. Ber.* 100 (1967) 3353; (d) W. Becker, W. Beck, H. Nöth, B. Wrackmeyer, *Chem. Ber.* 105 (1972) 2883.
- [7] (a) G.J. Bullen, N.H. Clark, *J. Chem. Soc. (A)* (1969) 404; (b) H. Nöth, R. Staudigl, W. Storch, *Chem. Ber.* 114 (1981) 3024; (c) H. Nöth, *Z. Naturforsch., Teil B* 38 (1983) 692; (d) G. Schmid, R. Boese, D. Blaeser, *Z. Naturforsch., Teil B* 37 (1982) 1230; (e) K.-H. van Bonn, P. Schreyer, P. Paetzold, R. Boese, *Chem. Ber.* 121 (1988) 1045; (f) H. Nöth, S. Weber, *Chem. Ber.* 117 (1984) 2504; (g) R. Boese, N. Niederprüm, D. Blaeser, *Struct. Chem.* 3 (1992) 399; (h) A. Hergel, H. Pritzkow, W. Siebert, *Angew. Chem.* 106 (1994) 1342; (i) A. Hergel, H. Pritzkow, W. Siebert, *Angew. Chem., Int. Ed. Engl.* 33 (1994) 1247; (j) H. Braunschweig, C.V. Koblinski, M. Mamuti, U. Englert, R. Wang, *Eur. J. Inorg. Chem.* (1999) 1899; (k) A. Berenbaum, H. Braunschweig, R. Dirk, U. Englert, J.C. Green, F. Jäkle, A.J. Lough, I. Manners, *J. Am. Chem. Soc.* 122 (2000) 5765.
- [8] (a) H. Werner, R. Prinz, E. Deckelmann, *Chem. Ber.* 102 (1969) 65; (b) G. Huttner, B. Krieg, *Angew. Chem.* 23 (1971) 541; (c) G. Huttner, B. Krieg, *Angew. Chem., Int. Ed. Engl.* 10 (1971) 512; (d) R. Köster, G. Seidel, B. Wrackmeyer, *Chem. Ber.* 122 (1989) 1825; (e) R. Köster, G. Seidel, B. Wrackmeyer, D. Schlosser, *Chem. Ber.* 122 (1989) 2055; (f) R. Köster, G. Seidel, C. Krüger, G. Müller, A. Jiang, R. Boese, *Chem. Ber.* 122 (1989) 2075.
- [9] B. Wrackmeyer, H.E. Maisel, M. Herberhold, *J. Organomet. Chem.* 637–639 (2001) 727.
- [10] B. Wrackmeyer, E.V. Klimkina, M. Herberhold, unpublished results.
- [11] (a) J.K.M. Sanders, B.K. Hunter, *Modern NMR Spectroscopy*, second ed., Oxford University Press, Oxford, 1993 (Chapter 6); (b) K. Stott, J. Keeler, Q. Van, A.J. Shaka, *J. Magn. Reson.* 125 (1997) 302.
- [12] J. Sandtsröm, *Dynamic NMR Spectroscopy*, Academic Press, New York, 1982, p. 96.
- [13] (a) H. Beall, C.H. Bushweller, *Chem. Rev.* 73 (1973) 465; (b) M. Oki, *Applications of Dynamic NMR Spectroscopy to Organic Chemistry*, VCH Publishers, Deerfield Beach, FL, 1985; (c) L. Lunazzi, C. Magagnoli, M. Guerra, D. Macciantelli, *Tetrahedron Lett.* (1979) 3031.
- [14] H. Nöth, B. Wrackmeyer, in: P. Diehl, E. Fluck, R. Kosfeld (Eds.), *Nuclear Magnetic Resonance Spectroscopy of Boron Compounds*, NMR – Basic Principles and Progress, vol. 14, Springer, Berlin, 1978, p. 171.
- [15] B. Jaschke, R. Herbst-Irmer, U. Klingebiel, T. Pape, *J. Chem. Soc., Dalton Trans.* (2000) 1827.
- [16] (a) M. Herberhold, in: A. Togni, T. Hayashi (Eds.), *Ferrocenes. Homogeneous Catalysis, Organic Synthesis, Materials Science*, VCH, Weinheim, 1995, pp. 219–278; (b) M. Herberhold, *Angew. Chem.* 107 (1995) 1985; (c) M. Herberhold, *Angew. Chem., Int. Ed. Engl.* 34 (1995) 1837.
- [17] (a) M. Herberhold, U. Dörfler, W. Milius, B. Wrackmeyer, *J. Organomet. Chem.* 492 (1995) 59; (b) K. Ma, H.-W. Lerner, S. Scholz, J.W. Bats, M. Bolte, M. Wagner, *J. Organomet. Chem.* 664 (2002) 94; (c) T. Moriuchi, I. Ikeda, T. Hirao, *Organometallics* 14 (1995) 3578; (d) M. Herberhold, U. Steffl, W. Milius, B. Wrackmeyer, *J. Organomet. Chem.* 533 (1997) 109.

- [18] M. Baudler, A. Marx, *Z. Anorg. Allg. Chem.* 474 (1981) 18.
- [19] (a) G.A. Morris, R. Freeman, *J. Am. Chem. Soc.* 101 (1979) 760;  
(b) G.A. Morris, *J. Am. Chem. Soc.* 102 (1980) 428;  
(c) J. Schraml, in: Z. Rappoport, Y. Apeloig (Eds.), *The Chemistry of Organic Silicon Compounds*, vol. 3, Wiley, Chichester, 2001, pp. 223–339.
- [20] K. Niedenzu, H. Beyer, J.W. Dawson, H. Jenne, *Chem. Ber.* 96 (1963) 2653.
- [21] (a) K. Niedenzu, J.W. Dawson, *J. Am. Chem. Soc.* 81 (1959) 5553;  
(b) H. Watanabe, K. Nagasawa, T. Totani, T. Yoshizaki, T. Nakagawa, O. Ohashi, M. Kubo, *Adv. Chem. Ser.* 42 (1964) 108.